



Graft Site Microenvironment Determines Dendritic Cell Trafficking Through the CCR7-CCL19/21 Axis

Citation

Hua, Jing, William Stevenson, Thomas H. Dohlman, Takenori Inomata, Maryam Tahvildari, Narghes Calcagno, Negar Pirmadjid, Zahra Sadrai, Sunil K. Chauhan, and Reza Dana. 2016. "Graft Site Microenvironment Determines Dendritic Cell Trafficking Through the CCR7-CCL19/21 Axis." *Investigative Ophthalmology & Visual Science* 57 (3): 1457-1467. doi:10.1167/iops.15-17551. <http://dx.doi.org/10.1167/iops.15-17551>.

Published Version

doi:10.1167/iops.15-17551

Permanent link

<http://nrs.harvard.edu/urn-3:HUL.InstRepos:29407768>

Terms of Use

This article was downloaded from Harvard University's DASH repository, and is made available under the terms and conditions applicable to Other Posted Material, as set forth at <http://nrs.harvard.edu/urn-3:HUL.InstRepos:dash.current.terms-of-use#LAA>

Share Your Story

The Harvard community has made this article openly available.
Please share how this access benefits you. [Submit a story](#).

[Accessibility](#)

Graft Site Microenvironment Determines Dendritic Cell Trafficking Through the CCR7-CCL19/21 Axis

Jing Hua, William Stevenson, Thomas H. Dohlman, Takenori Inomata, Maryam Tahvildari, Narghes Calcagno, Negar Pirmadjid, Zahra Sadrai, Sunil K. Chauhan, and Reza Dana

Schepens Eye Research Institute, Massachusetts Eye and Ear Infirmary, Department of Ophthalmology, Harvard Medical School, Boston, Massachusetts, United States

Correspondence: Reza Dana, Schepens Eye Research Institute, 20 Staniford Street, Boston, MA 02114, USA; reza_dana@meei.harvard.edu.

Submitted: June 23, 2015
Accepted: February 14, 2016

Citation: Hua J, Stevenson W, Dohlman TH, et al. Graft site microenvironment determines dendritic cell trafficking through the CCR7-CCL19/21 axis. *Invest Ophthalmol Vis Sci*. 2016;57:1457–1467. DOI:10.1167/iov.15-17551

PURPOSE. The graft site microenvironment has a profound effect on alloimmunity and graft survival. We aimed to study the kinetics and phenotype of trafficking antigen-presenting cells (APC) to the draining lymph nodes (DLNs) in a mouse model of corneal transplantation, and to evaluate the homing mechanisms through which graft site inflammation controls APC trafficking.

METHODS. Allogeneic donor corneas were transplanted onto inflamed or quiescent graft beds. Host- (YAc⁺) and donor (CD45.1⁺ or eGFP⁺)-derived APCs were analyzed by flow cytometry. Protein and mRNA expression of the CC chemokine receptor (CCR)7 ligands CCL19 and CCL21 were assessed using ELISA and Real-Time qPCR, respectively. Transwell migration assay was performed to assess the effect of DLNs isolated from hosts with inflamed graft beds on mature bone marrow-derived dendritic cells (BMDCs).

RESULTS. We found that inflamed graft sites greatly promote the trafficking of both recipient- and graft-derived APCs, in particular mature CCR7⁺ CD11c⁺ dendritic cells (DC). CCL19 and CCL21 were expressed at significantly higher levels in the DLNs of recipients with inflamed graft beds. The supernatant of DLNs from recipients with inflamed graft beds induced a marked increase in mature DC migration compared with supernatant from recipients with quiescent graft beds in a transwell assay. This effect was abolished by neutralizing CCL19 or CCL21. These data suggest that graft site inflammation increases the expression of CCR7 ligands in the DLNs, which promote mature DC homing and allojection.

CONCLUSIONS. We conclude that the graft site microenvironment plays a critical role in alloimmunity by determining DC trafficking through the CCR7-CCL19/21 axis.

Keywords: antigen presenting cells, migration, microenvironment, CCR7, CCL19, CCL21

Clinical and experimental findings indicate that transplant survival is influenced by the graft bed microenvironment, and strategies that alter this microenvironment (e.g., suppressing the host bed inflammation prior to transplantation) may improve graft survival. This concept has received support from earlier findings in experimental corneal transplantation that suggest the graft site microenvironment can have a profound effect on alloimmunity.^{1–3} Accordingly, corneal transplantation into inflamed or vascularized corneal beds is recognized as a ‘high-risk’ transplant with a survival rate between 35% and 65% in the first year,^{1,4–6} despite maximal use of both local and systemic immunosuppressive drugs, while corneas transplanted into quiescent graft beds yield a 2-year survival rate greater than 90% without systemic immunosuppression,^{6,7} highlighting the importance of perioperative inflammation in the development of alloimmunity. In corneal transplantations performed in quiescent ‘low-risk’ graft beds, the indirect sensitization pathway is dominant^{8–12}; however, in ‘high-risk’ inflamed graft site, the direct pathway of sensitization becomes predominant.³ The degree and kinetics of sensitization is determined in part by the phenotype and maturation status of antigen presenting cells (APC).^{13–16} Increased allosensitization in hosts with inflamed graft beds leads to higher graft rejection rates compared with hosts with quiescent graft beds.¹⁷ However, the molecular

mechanisms mediating increased allosensitization and graft rejection in inflamed hosts remain to be fully elucidated.

CC chemokine receptor (CCR) 7 knock out in donor-derived APCs leads to reduced allosensitization¹⁸ and cell trafficking,¹⁹ suggesting a critical role of CCR7-mediated APC trafficking in transplantations carried out in inflamed graft beds. The homing factors for CCR7-mediated cell trafficking are CC chemokine ligand (CCL) 19 and CCL21,²⁰ and their expression can be increased due to tissue inflammation.²¹ Thus, we hypothesize that graft site inflammation determines the trafficking of corneal APCs by regulating CCL19 and CCL21 expression in DLN.

In the current study, we used a murine corneal transplantation model and systematically analyzed the kinetics and phenotype of trafficking host- and donor-derived APCs at various time points. Our results suggest that an inflamed graft site microenvironment leads to increased expression of CCR7 ligands in the DLNs, promoting mature APCs to migrate to the DLNs, and thus amplifying allosensitization and graft rejection.

MATERIALS AND METHODS

Mice

Six-week-old male BALB/c and C57BL/6 mice were purchased from Charles River Laboratories (Wilmington, MA, USA). The



eGFP⁺ transgenic (CByJ.B6-Tg[CAG-EGFP]10sb/J) and CD45.1⁺ transgenic (B6.SJL-Ptprc^aPep3^b/BoyJ) mice were from Jackson Laboratory (Bar Harbor, ME, USA). Two donor-recipient combinations were used for tracing the trafficking APCs: donor corneas from eGFP⁺ mice were transplanted onto BALB/c recipients to measure the eGFP⁺ donor APC trafficking; CD45.2⁺ wild-type BALB/c donor grafts were transplanted to transgenic CD45.1⁺ recipients to measure CD45.2⁺ donor APCs, and YAc⁺ recipient APCs. All animals were treated in accordance with the ARVO statement for the Use of Animals in Ophthalmic and Vision Research, and experiments were approved by the Institutional Animal Care and Use Committee.

Corneal Transplantation

As previously described,^{17,22,23} inflamed graft beds were created by placing three intrastromal 11-0 nylon sutures (Sharp; Surgical Specialties Corporation, Reading, PA, USA) into the central cornea of recipient eye 14 days before transplantation. These sutures reliably induce neovascularization.²² During transplantation (day 0), a 2-mm corneal button was harvested from the donor animal and grafted onto an inflamed or quiescent 1.5-mm graft bed with eight interrupted 11-0 nylon sutures. Intraperitoneal ketamine (120 mg/kg) and xylazine (20 mg/kg) were used for anesthesia with additional perioperative subcutaneous buprenorphine (0.1 mg/kg).

Flow Cytometry

Draining lymph nodes were excised at 4, 24, 48, and 72 hours after corneal transplantation, and 2×10^6 cells from single cell suspension were used for flow analysis. The CD90.2⁺ fraction was isolated using magnetic-activated cell sorting (MACS; #130-094-523; Miltenyi Biotec, Auburn, CA, USA) as indicated. After incubation in FcReceptor-blocker (R&D Systems, Minneapolis, MN, USA), cells were incubated with following antibodies and isotype controls (Biolegend, San Diego, CA, USA; unless noted): FITC anti-mouse Ea52-68 peptide bound to I-A^b (YAc, clone eBioYAc; eBioscience, San Diego, CA, USA), Alexa Fluor647 anti-mouse CD3 ϵ antibody (clone 145-2C11), PE anti-mouse CD45.1 (clone A20), Alexa Fluor488 anti-eGFP (clone A-21311; Invitrogen, Grand Island, NY, USA), FITC and Alexa Fluor647 anti-mouse/human CD11b antibody (clone M1/70), PECy5 and FITC anti-mouse CD11c (clone N418; eBioscience), PE/Cy7 anti-mouse I-A/I-E antibody (MHC II, clone M5/114.15.2), and PE anti-mouse CD197 (CCR7) antibody (clone 4B12). Stained cells were analyzed using the LSR II flow cytometer (BD Bioscience, San Jose, CA, USA) and FlowJo software (Tree Star, Ash Island, OR, USA). YAc mAb recognizes the epitope defined by donor MHC class II I-Ea 52-68 peptide presented in the context of recipient MHC class II I-A^d.^{24,25} Upon transplantation of CD45.2⁺ BALB/c donor corneas to CD45.1 C57BL/6 recipients, recipient-derived cells (I-A^d) capture and process donor MHC class II (I-E), and present the I-Ea 52-68 peptide, thus becoming YAc⁺ alloantigen-bearing recipient-derived APCs.

RNA Isolation and Quantitative Real-Time PCR

Draining lymph nodes were snap-frozen in liquid nitrogen; RNA was isolated using the RNeasy Mini Kit (Qiagen, Germantown, MD, USA), and reverse transcribed using oligo (dT) primer and SuperscriptTM III (Invitrogen). One microliter of total cDNA synthesized from 400 ng of total RNA was used for each quantitative Real-Time PCR ($n = 6$ /group) with Taqman Universal PCR Mastermix and FAM-MGB dye-labeled, predesigned gene expression assays (Applied Biosystems, Foster City, CA, USA) for *Ccl19* (Mm00839967_g1) and *Gapdh*

(Mm99999915_g1). *Ccl21*^{Ser} primers were synthesized according to verified sequences (Harvard PrimerBank ID: 14547891a1). The results were analyzed using the comparative threshold cycle (C_T) method.

Enzyme-Linked Immunosorbent Assay

Draining lymph nodes from recipients with inflamed and quiescent graft beds were collected 24 hours after corneal transplantation ($n = 3$ /group), and protein was extracted in radioimmunoprecipitation assay (RIPA) buffer containing proteinase inhibitor cocktail (Roche, Indianapolis, IN, USA), 10 mM NaF, and 1 mM Na₃VO₄ (Sigma-Aldrich Corp., St. Louis, MO, USA). In addition, sorted CD11c⁺ cells were cultured 0.5×10^6 /mL in media containing phorbol 12-myristate 13-acetate (PMA) and ionomycin (Sigma-Aldrich Corp.) for 24 hours in a U-bottom 96-well culture plate, and the supernatant of the cell culture was then used for ELISA ($n = 5$ /group). For each ELISA reaction, 1000 ng total protein was used (concentration measured by BCA assay; Pierce, Rockford, IL, USA) in detection kits for murine CCL19/MIP-3 β and CCL21/6CKine (R&D Systems). Absorbance was determined using a POLARstar Optima plate reader (BMG Labtech; Cary, NC).

Culture of BMDCs

Bone marrow-derived dendritic cells were cultured as previously described.²⁶ To generate mature BMDCs, immature BMDCs were subcultured in 6-well plates with 10 ng/mL of IFN- γ (PeproTech, Rocky Hill, NJ, USA) for 48 hours.

Ex Vivo Draining Lymph Node Explant Culture

Ipsilateral DLNs from recipients with inflamed and quiescent graft beds were collected at 24 hours after corneal transplantation, and incubated with 500 μ L of supplemented RPMI-1640 medium (PMA/Ionomycin; Sigma-Aldrich Corp.) at 37°C for 24 hours. Supernatant was then collected for the migration assays.

Transwell Migration Assay and In Vitro Chemokine Neutralization

The BMDC migration assay was performed with transwell inserts with polycarbonate filters (5- and 8- μ m pore size for immature BMDCs; 8 μ m for mature BMDCs; Corning Life Sciences, Tewksbury, MA, USA). Mature BMDCs at 1×10^5 were placed in the top well. As a potential source of chemotactic stimuli, serial dilutions and/or 200 μ L of DLN culture supernatant from recipients with inflamed and quiescent graft beds was added to each well (two independent experiments with $n = 3$ mice/group). Single or a combination of neutralization antibodies against CCL19 (10 μ g/mL) and CCL21 (2 μ g/mL; AF880, AF457; R&D Systems) was added to the bottom wells as indicated. Additional control wells with matching isotypes and lipopolysaccharide (LPS) were used. To assess a possible toxic effect of neutralizing antibodies, we assessed cell viability using trypan blue staining before and 4 hours after treatment with antibodies. In a second transwell migration experiment, mature BMDCs were stimulated with IFN- γ and treated with or without dexamethasone (10^{-7} M) and supernatant.²⁷ Additionally, we added anti-CCL19 and anti-CCL21 at different concentrations to determine the additive effect in suppressing DC migration. After incubation for 4 hours at 37°C, green fluorescent microspheres (1×10^5 /well; Dako, Carpinteria, CA, USA) were added to each well as an internal control.

Samples were analyzed using flow cytometry with a stopping gate at 0.5×10^5 microsphere counts.

Statistical Analyses

Experiments with more than two groups were analyzed via 1- or 2-way ANOVA test with post hoc Tukey's or Bonferroni's multiple comparison test. Comparisons between two groups were analyzed using the Student's *t*-test. A *P* value of less than 0.05 was considered statistically significant. All statistical calculations were performed using Prism Version 5.04 software (GraphPad, La Jolla, CA, USA).

RESULTS

Inflammation in the Graft Beds Increases Homing of Graft-Derived APCs to DLNs

In order to identify graft-derived APCs, we transplanted eGFP⁺ transgenic corneal grafts (C57BL/6) onto BALB/c host beds, or CD45.2⁺ grafts (BALB/c) onto transgenic CD45.1⁺ C57BL/6 hosts. To achieve a more distinct separation of graft cell population, we depleted CD90.2⁺ lymphocytes in the eGFP⁺ grafted recipient samples prior to flow cytometry analysis (Fig. 1A). In CD45.1⁺ recipients with CD45.2⁺ corneal grafts, cells were stained with anti-CD45.2 and anti-CD3 antibodies, and then gated on CD45.2⁺CD3⁻ cells (Fig. 1C). Between 4 and 72 hours post transplantation, we observed increased frequencies of graft-derived APCs (eGFP⁺ and CD45.2⁺) trafficking to the DLNs in recipients with inflamed graft beds compared with recipients with quiescent graft beds, with a peak at 24 hours (Figs. 1B, 1D).

Inflamed Graft Beds Enhance Homing of Recipient Alloantigen-Bearing APCs to DLNs

After transplantation of CD45.2⁺ Balb/c corneas into inflamed or quiescent graft beds of CD45.1⁺ C57BL/6 hosts, we detected recipient alloantigen-bearing APCs (CD3⁻YAc⁺) in DLNs using flow cytometry (Fig. 1E). Recipients with inflamed graft beds displayed significantly higher frequencies of CD3⁻YAc⁺ cells in the DLNs than recipients with quiescent graft beds as early as 4 hours; this was sustained until 48 hours post grafting, and slightly decreased at 72 hours, while the frequencies of CD3⁻YAc⁺ cells in recipients with quiescent graft beds progressively increased between 4 and 72 hours (Fig. 1F).

Inflamed Graft Beds Increase MHC II⁺CCR7⁺ DC Homing to the DLNs

Next, we analyzed the expression of MHC II and CCR7 on trafficking eGFP⁺ graft-derived and YAc⁺ host-derived APCs to the DLNs 24 hours post transplantation (Fig. 2). The total cell count of eGFP⁺ and YAc⁺ cells was increased in the DLNs of recipients with inflamed graft beds (Figs. 2A, 2B). Transplantations into inflamed graft beds led to a significant increase of MHC II⁺CCR7⁺ cells of both eGFP⁺ (Figs. 2C, 2D) and YAc⁺ (Figs. 2E, 2F) cells in the DLNs compared with transplantations into quiescent graft beds. Further analysis of CD11c and CD11b expression on APCs revealed that the frequencies of both CD11c⁺CD11b⁻ Langerhans cells and CD11c⁺CD11b⁺ DCs were increased among eGFP⁺ graft-derived APCs (Figs. 2G–I), and the frequencies of CD11c⁺CD11b⁺ DCs among YAc⁺ host-derived APCs were significantly increased in the DLNs of recipients with inflamed graft beds (Figs. 2J–L).

CCL19 and CCL21 Expression are Upregulated in DLNs After Transplantation Into Inflamed Graft Beds

We assessed mRNA expression of a series of chemokines including CCL1, CCL2, CCL19, and CCL21, and CXCL13, and found that the CCR7 ligands CCL19 and CCL21 were significantly upregulated in the DLNs of recipients with inflamed graft beds (Fig. 3A), while their expression levels in other lymphoid tissues such as the spleen and thymus were comparable in both conditions (Supplementary Material S1). Using ELISA assays, we found that the protein levels of the CCR7 ligands in the DLNs of recipients with inflamed graft beds were significantly higher than in the DLNs of recipients with quiescent graft beds. No significant difference was detected between naïve mice and recipients with quiescent graft beds (Fig. 3B).

CD11c⁺ Dendritic Cells in Inflammation Contribute to the Enhanced Secretion of CCL19 and CCL21 in DLNs

We first analyzed the maturation status of total CD11c⁺ cells, and found that CD11c⁺ DCs from recipients with inflamed graft beds displayed higher frequencies of MHC II^{hi} cells and an overall increased level of MHC II protein expression compared to DCs from recipients with quiescent graft beds (Fig. 3C). After sorting CD11c⁺ DCs from the DLNs of recipients with inflamed and quiescent graft beds, we cultured these cells for 24 hours under stimulation, and then measured the protein level of CCL19 and CCL21 in the culture supernatant using ELISA. We found that CD11c⁺ cells from DLNs of recipients with inflamed graft beds secreted significantly higher amounts of both CCL19 and 21 than CD11c⁺ cells from recipients with quiescent graft beds (Fig. 3D).

Increased CCL19 and CCL21 Secretion Selectively Recruits More Mature Dendritic Cells In Vitro

To evaluate the chemotactic ability of secreted factors from the DLNs after transplantation, we used mature BMDCs in a transwell migration assay, and assessed the number of migrated cells toward the supernatant from DLNs of recipients with inflamed versus quiescent graft beds. Culture supernatant of DLNs explanted from the recipients with inflamed graft beds significantly increased the numbers of migrating mature BMDCs (Supplementary Material S2B). Next, we determined mature BMDC migration after neutralization of CCL19 or CCL21 with murine antibodies in the supernatant of recipients with inflamed graft beds. Both CCL19 and CCL21 neutralization alone or in combination reduced BMDC migration compared with BMDCs with supernatant only (Fig. 4A). Because cell viability before and after the assay was similar in all groups (>97%), reduced cell numbers are due to decreased migration and not cell death. Mature BMDCs used in this transwell assay exhibited higher levels of CCR7 and MHC II compared with immature BMDCs (Fig. 4B).

Because immunosuppressive treatment is known to inhibit DC maturation,²⁸ we next determined whether the blockade of CCL19 and CCL21 can alter the response to immunosuppression with dexamethasone, a commonly used corticosteroid in humans. We used the transwell system and analyzed the migration potential of BMDCs after immunosuppression with dexamethasone in combination with or without neutralizing CCL19 and CCL21. As expected, dexamethasone alone significantly decreased the number of migrated BMDCs. Moreover, additional treatment with anti-CCL19 and anti-

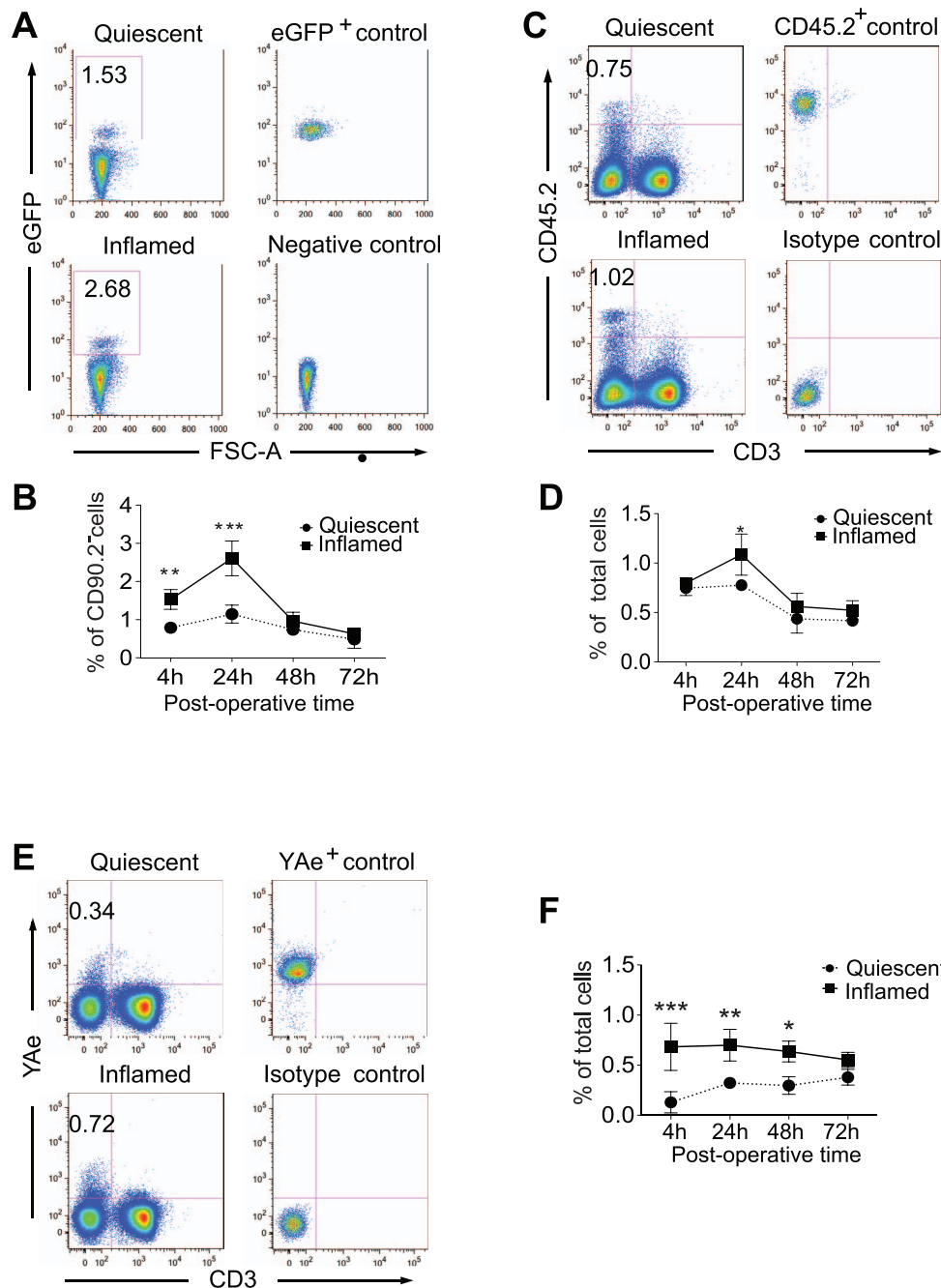


FIGURE 1. Kinetics of trafficking host- and donor-derived APCs to the DLN. Allogeneic donor corneas were transplanted into the recipients had inflamed or quiescent graft beds. Inflamed graft beds were created by placing intrastromal corneal sutures. Single cell suspensions from the DLNs of recipients were analyzed at various time points post transplantation using flow cytometry. **(A)** To assess donor-derived APCs, corneas of eGFP⁺ C57BL/6 were transplanted onto BALB/c mice with inflamed or quiescent graft beds. Representative analysis shows eGFP⁺ donor-derived APCs in the lymph nodes at 24 hours post operation. To exclude donor-derived T cells, CD90.2⁺ cells were depleted before flow cytometry analysis. Cell numbers, 4 hours: 4.4 ± 0.1 vs. 4.5 ± 0.08 ; 24 hours: 4.4 ± 0.1 vs. 4.4 ± 0.1 ; 48 hours: 4.4 ± 0.08 vs. 4.3 ± 0.08 ; and 72 hours: 4.6 ± 0.03 vs. 4.5 ± 0.1 ($\times 10^6$ /sample). **(B)** Frequencies of eGFP⁺ donor cells at 4, 24, 48, and 72 hours in the DLNs after corneal transplantation are shown (** $P < 0.001$, *** $P < 0.0001$, $n = 3$ /group, 2-way ANOVA, Bonferroni post test, 1×10^6 events/sample). **(C)** To assess donor-derived APCs, CD45.2⁺ BALB/c donors were transplanted onto transgenic CD45.1⁺ C57BL/6 mice with inflamed or quiescent graft beds. Representative analysis shows CD45.2⁺ CD3⁻ donor-derived APCs in the lymph nodes at 24 hours post operation. Cell numbers, 4 hours: 7.9 ± 0.2 vs. 8.1 ± 0.3 ; 24 hours: 8.2 ± 0.2 vs. 8.0 ± 0.1 ; 48 hours: 8.0 ± 0.004 vs. 8.0 ± 0.1 ; and 72 hours: 8.0 ± 0.004 vs. 8.0 ± 0.003 ($\times 10^6$ /sample). **(D)** Frequencies of CD45.2⁺CD3⁻ donor APCs at 4, 24, 48, and 72 hours in the DLNs after corneal transplantation are shown (* $P < 0.05$, $n = 3$ /group, 2-way ANOVA, Bonferroni post test, 1×10^6 events/sample). **(E)** To assess alloantigen-bearing host-derived APCs, cells were stained for YAc expression in transgenic CD45.1⁺ C57BL/6 hosts who had received CD45.2⁺ BALB/c donor corneas. To exclude T cells, the cells were stained for CD3 expression. Representative analysis shows host-derived YAc⁺CD3⁻ APCs distributed in lymph nodes at 24 hours post transplantation. Cell numbers, 4 hours: 7.9 ± 0.2 vs. 8.1 ± 0.1 ; 24 hours: 8.1 ± 0.2 vs. 8.1 ± 0.2 ; 48 hours: 8.0 ± 0.2 vs. 8.0 ± 0.2 ; and 72 hours: 8.0 ± 0.1 vs. 8.1 ± 0.1 ($\times 10^6$ /sample). **(F)** Frequencies of YAc⁺CD3⁻ cells at 4, 24, 48, and 72 hours after corneal transplantation are shown (Values are expressed as mean \pm SEM, * $P < 0.05$, ** $P < 0.01$, *** $P < 0.001$; $n = 4$, 2-way ANOVA, Bonferroni post test, 1×10^6 events/sample). Representative results from at least three repeats at each time point.

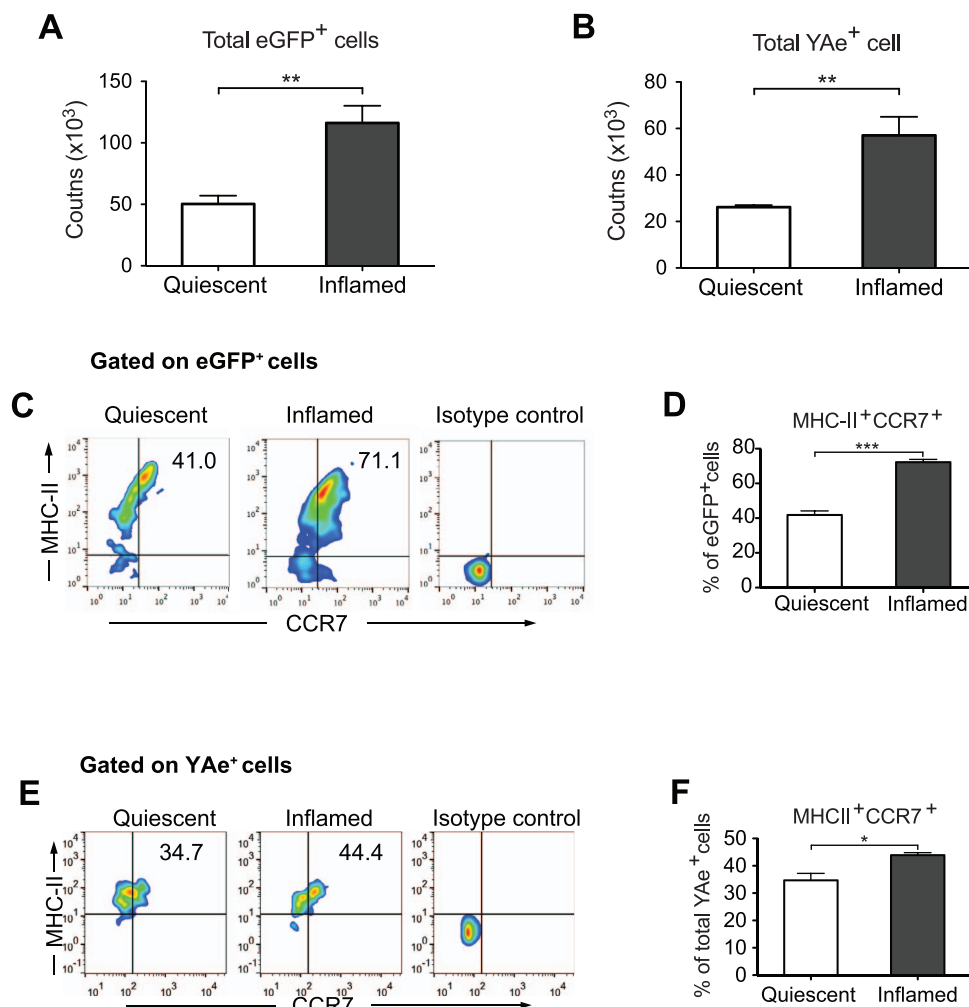


FIGURE 2. Phenotypic analysis of donor-derived APCs in DLNs at 24 hours post transplantation. Total cell numbers of (A) eGFP⁺ donor-derived (50.28 ± 6.83 vs. 116.1 ± 14.05 [$\times 10^3$ /sample], $n = 3$, $P = 0.0103$, t -test) and (B) YAc⁺ host-derived cells (26.17 ± 0.89 vs. 57.03 ± 8.07 [$\times 10^3$ /sample], $n = 3$, $P = 0.0094$, t -test) in DLNs are shown 24 hours after transplantation. (C) Representative dot plot graph showing trafficking eGFP⁺ cells analyzed for CCR7 and MHC II expression in the DLNs of recipients with inflamed and quiescent graft beds using flow cytometry. (D) Frequencies of MHC II⁺CCR7⁺ donor-derived cells in the lymph nodes of recipients with inflamed graft beds compared with recipients with quiescent graft beds are shown (72.2 ± 1.6 vs. $41.8 \pm 2.3\%$, $n = 3$ /group, $***P < 0.0001$, Student's t -test). (E) Representative dot plot graph shows trafficking host-derived YAc⁺ cells analyzed for CCR7 and MHC II expression in the DLNs of recipients with inflamed and quiescent graft beds using flow cytometry. (F) Frequencies of MHC II⁺CCR7⁺ host-derived cells in the lymph nodes of recipients with inflamed graft beds compared with recipients with quiescent graft beds are shown (34.7 ± 2.6 vs. $43.9 \pm 0.9\%$, $n = 3$ /group, $*P = 0.03$, Student's t -test). (G) Representative dot plot graph showing eGFP⁺ donor-derived cells from recipient lymph nodes analyzed for CD11b and CD11c expression. (H) Frequencies of CD11c⁺CD11b⁺ donor-derived dendritic cells in the lymph nodes of recipients with inflamed and quiescent graft beds are shown (29.1 ± 4.3 vs. $45.9 \pm 3.0\%$, $n = 3$ /group, $*P = 0.03$, Student's t -test). (I) Frequencies of CD11c⁺CD11b⁺ donor-derived dendritic cells in the lymph nodes of recipients with inflamed and quiescent graft beds are shown (12.2 ± 1.3 vs. $21.7 \pm 2.6\%$, $n = 3$ /group, $*P = 0.03$, Student's t -test). (J) Representative dot plot graph showing YAc⁺ host-derived cells from recipient lymph nodes analyzed for CD11b and CD11c expression. (K) Frequencies of CD11c⁺CD11b⁺ host-derived dendritic cells in the lymph nodes of recipients with inflamed and quiescent graft beds are shown (72.0 ± 2.5 vs. $65.6 \pm 1.0\%$, $n = 3$ /group, n.s. $P = 0.08$, Student's t -test). (L) Frequencies of CD11c⁺CD11b⁺ host-derived dendritic cells in the lymph nodes of recipients with inflamed and quiescent graft beds are shown (11.0 ± 0.6 vs. $19.17 \pm 0.9\%$, $n = 3$ /group, $**P = 0.0017$, Student's t -test).

CCL21 further decreased cell migration in a dose-dependent manner (Fig. 4C).

DISCUSSION

Inflammation at transplant site determines allorecognition.³ We aimed to investigate whether allorecognition is mediated through regulating mature APC trafficking via the CCR7-CCL19/21 axis. The importance of APC trafficking has been shown in various transplantation settings,^{25,29,30} and studies in corneal transplantation suggest that inflamed graft beds are

associated with enhanced trafficking of APCs to lymphoid tissue.^{1,23} However, most studies reported their findings at a single time point that varies from study to study, and very little is known about the mechanisms how the graft site microenvironment regulates APC trafficking. The inflammatory cytokines TNF- α and IL-1 have been shown to promote DC maturation and allosensitization,³¹ and blocking these cytokines improves graft survival.³²⁻³⁵ Dendritic cell homing is mostly dependent on CCR7,³⁶ and mature DCs express CCR7 by which they sense CCL21 gradients, allowing them to migrate to lymphatic vessels, both in steady state and in inflammation.³⁷ To clarify previous findings, and determine a

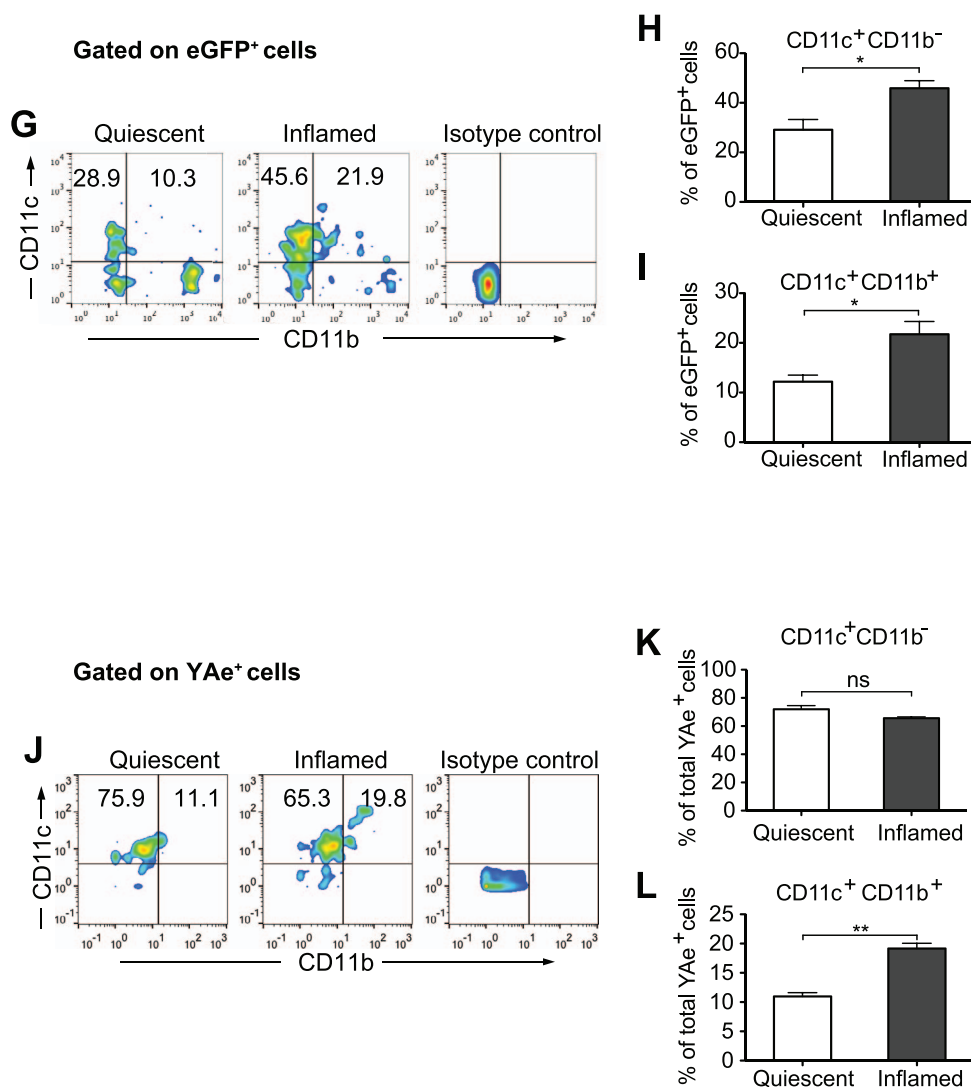


FIGURE 2. Continued.

suitable time point to analyze the homing mechanisms, we performed a systematic analysis of the kinetics and magnitude of the trafficking APCs in high-risk recipients with inflamed graft beds versus low-risk recipients with quiescent graft beds. Our results indicate that the CCR7 ligands CCL19 and CCL21 are significantly upregulated in DLNs of high-risk recipients and are principally involved in promoting graft site APC trafficking to host lymphoid tissues, thus amplifying allorecognition.

Previous studies have mainly used MHC II allopeptides (I-A^d or I-A^b) to identify recipient- and donor-derived APCs. There are significant limitations with this method, because the expression levels of MHC II vary dramatically depending on cell type and maturation; I-A^{d+} cells in a BALB/c recipient do not all present alloantigens; and in normal donor APCs,^{1,23,28} I-A^b is highly expressed only after inflammatory stimulation in corneal DCs.³⁸ Here, we used YAc staining (YAc⁺CD3⁻) to detect recipient APCs bearing alloantigen, which identifies the recipient MHC II molecules that bear processed donor I-Ea 52-68 peptide.²⁵ Further, we used eGFP⁺ or CD45.2⁺ grafts to trace donor-derived APCs. We observed significantly higher frequencies of recipient- and donor-derived APCs in the DLNs of recipients with inflamed graft beds than quiescent graft beds. The increase of trafficking

APCs observed in our study confirms previous findings in high-risk recipients,³ and further suggests that the increased APC frequencies may lead to higher allosensitization. In addition, the kinetics and magnitude of trafficking APCs in recipients with quiescent graft beds was consistent with previous reports in corneal and other organ transplantation models at the respective time points.^{25,29,30}

We further focused on these cells for phenotypic analyses and observed that the frequencies of mature MHC II⁺CCR7⁺ and CD11c⁺CD11b⁻ DCs were significantly higher in the DLNs of recipients with inflamed graft beds, suggesting that inflammation leads to a selective recruitment of mature DCs to the DLNs. The increase of mature DCs in the DLNs of recipients with inflamed graft beds strongly indicates their role in enhancing allosensitization and graft rejection. The higher frequencies of CCR7⁺ APCs in the DLNs after transplantation into inflamed graft beds also suggest that CCR7 plays a critical role in homing of these cells to the DLNs. In fact, we observed a significant increase of mRNA and protein expression for both CCR7 ligands, CCL19 and CCL21, in recipients with inflamed graft beds, suggesting that trafficking of mature DCs from the inflammatory graft site to the DLNs is mediated through their increased secretion. In inflammation, lymphotoxin alpha/beta, and TNF are known to upregulate CCL19 and CCL21

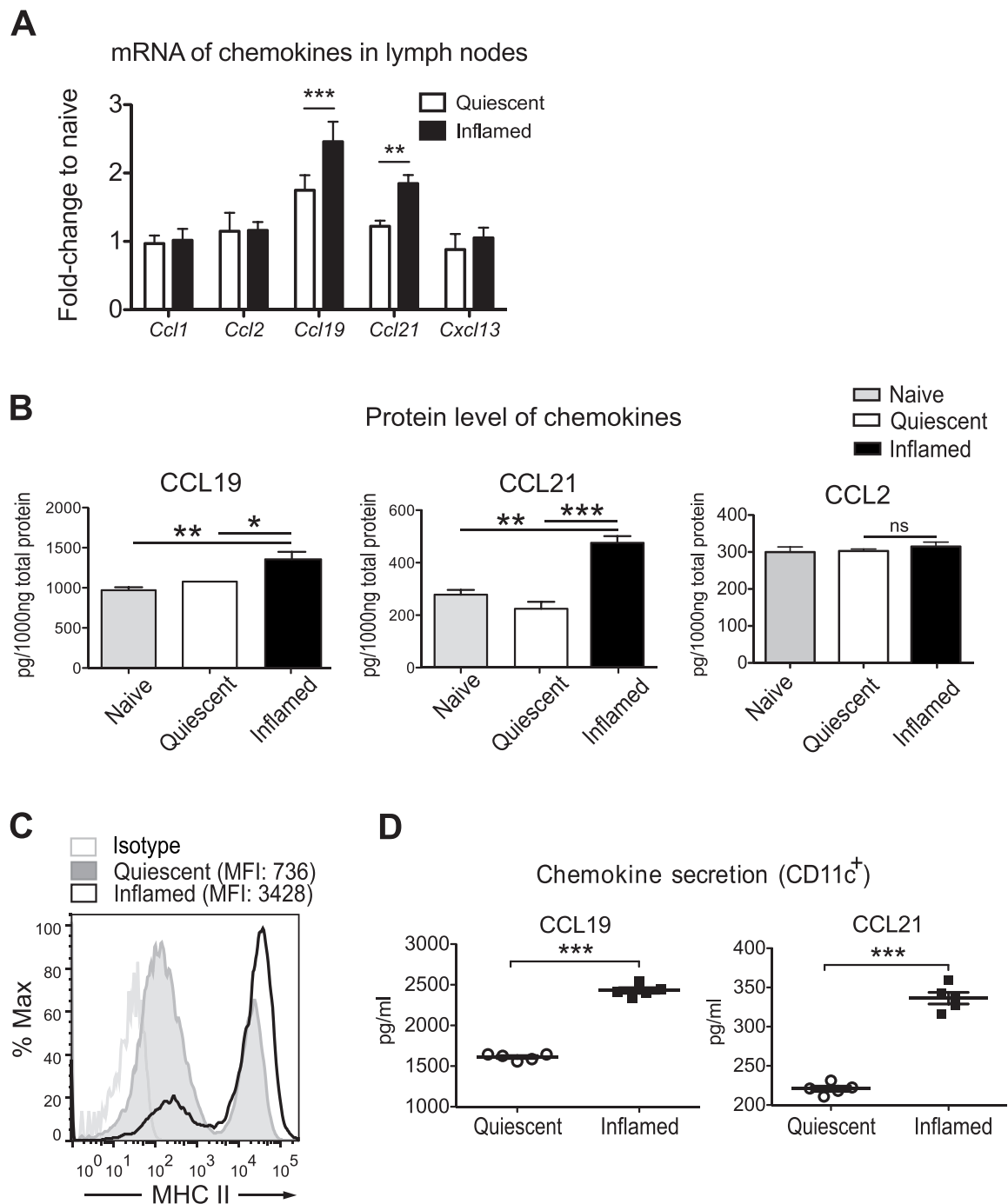


FIGURE 3. Transplantation in inflamed graft beds enhances CCL19 and CCL21 secretion in the lymph nodes and dendritic cells. (A) The mRNA expression of *Ccl1*, *Ccl2*, *Ccl19*, *Ccl21*, and *Cxcl13* in lymph nodes of recipients with inflamed and quiescent graft beds was quantified at 24 hours post transplantation using Real-Time qPCR (** $P < 0.01$, *** $P < 0.001$; $n = 6/\text{group}$, 2-way ANOVA, Bonferroni post test). A primer pair designed for *Ccl21*^{Ser} was used here, because murine lymph nodes only express CCL21^{Ser}.⁵⁸ (B) Protein expression of CCL19, CCL21, and CCL2 in the lymph nodes of recipients with inflamed and quiescent host beds as well as naïve mice was measured in tissue lysates using ELISA 24 hours post transplantation. (CCL19: 1356 ± 94 vs. 1065 ± 18 and 971.7 ± 63 pg/mg total protein, $n = 3/\text{group}$, $P = 0.008$, CCL21: 475.5 ± 25.8 vs. 223.1 ± 45.8 and 278.4 ± 18.0 pg/mg total protein, $n = 3/\text{group}$, *** $P = 0.0007$, 1-way ANOVA with post hoc Tukey's test, * $P < 0.05$, ** $P < 0.001$, *** $P < 0.0001$). (C) Representative flow cytometry analysis showing MHC II expression of sorted CD11c⁺ cells of DLNs of recipients with inflamed and quiescent graft beds 24 hours after transplantation ($n = 6/\text{group}$). (D) Protein expression of CCL19 and CCL21 of sorted CD11c⁺ cells was measured by ELISA 24 hours post transplantation. CD11c⁺ cells isolated from lymph nodes of recipients with inflamed and quiescent graft beds were cultured with PMA and ionomycin and the supernatant was collected after 24 hours (CCL19: 1612 ± 17 vs. 2430 ± 34 , $n = 5/\text{group}$, *** $P < 0.0001$; CCL21: 220.7 ± 3.3 vs. 336.2 ± 7.4 , $n = 5/\text{group}$, *** $P < 0.0001$).

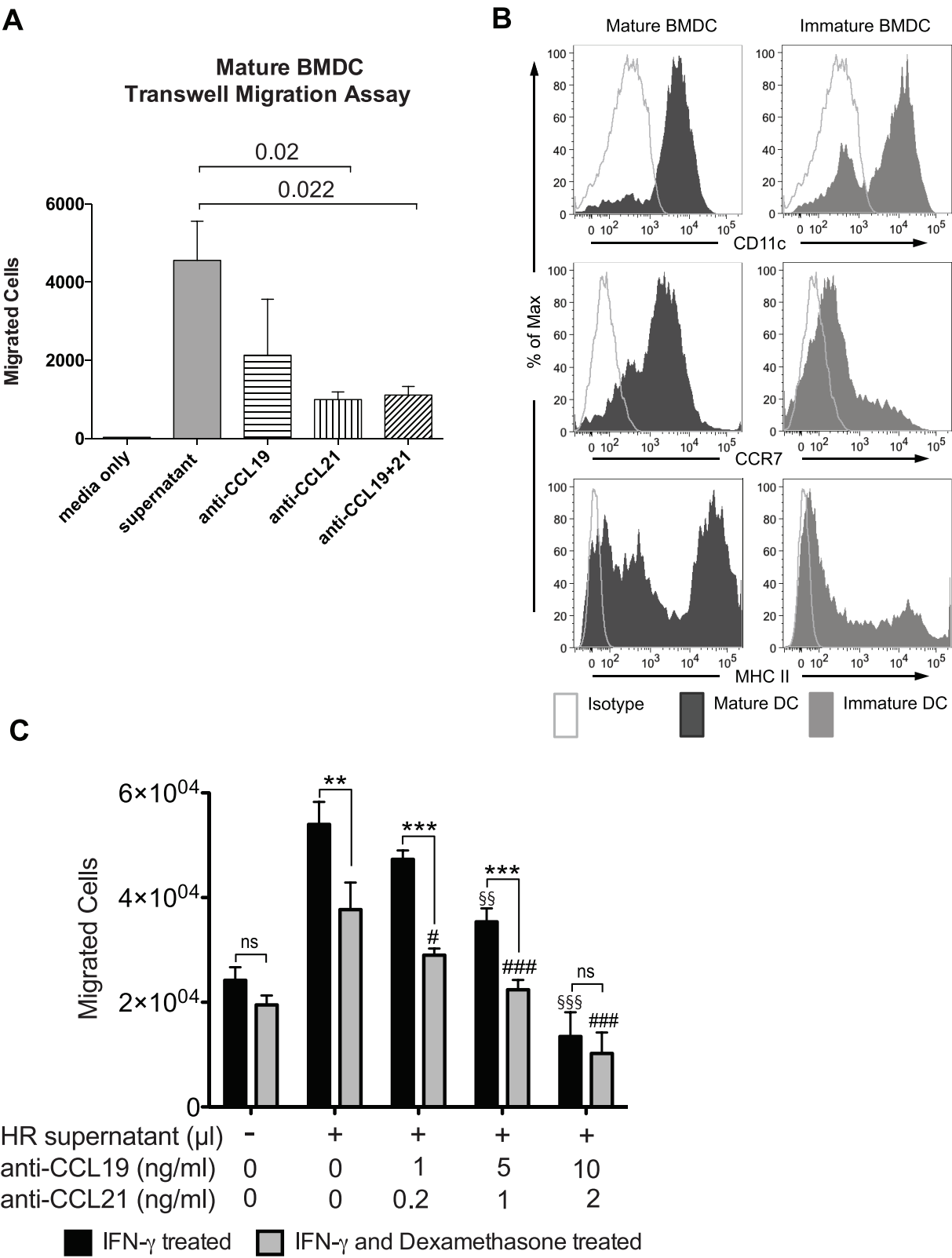


FIGURE 4. Increased CCL19 and CCL21 expression in lymph nodes of recipients with inflamed graft beds promotes mature dendritic cell migration. (A) For the transwell migration assay 200 μ L supernatant of cultured lymph nodes isolated from recipients with inflamed graft beds were added to the bottom well as a chemoattractant, and mature BMDCs were added to the upper well. Neutralizing antibodies against CCL19 (10 μ g/mL) and/or CCL21 (2 μ g/mL) were added as indicated (data show results from one out of two experiments with 3 mice/each group; Student's *t*-test). (B) Representative flow cytometry analysis showing CD11c, CCR7, and MHC II expression of mature and immature BMDCs used in the transwell assay (data from one out of three independent experiments are shown). (C) Transwell migration assay with mature BMDCs cultured with supernatant from lymph nodes of recipients with inflamed graft beds. Bone marrow-derived dendritic cells were stimulated with IFN- γ with or without

dexamethasone. Anti-CCL19 and anti-CCL21 antibodies were added at different concentrations as indicated. $^{**}P < 0.001$, $^{***}P < 0.0001$ (IFN- γ treated versus IFN- γ and dexamethasone treated); $^{\#}P < 0.05$, $^{###}P < 0.0001$ (compared with IFN- γ and dexamethasone-treated samples with supernatant but no neutralizing antibodies), $^{\$}P < 0.001$, $^{\$ \$ \$}P < 0.0001$ (compared with IFN- γ treated samples with supernatant but no neutralizing antibodies).

production.^{39–43} Mature DCs can alter the secretion of chemokines in high endothelial venules (HEV) and fibroblastic cells, and DC-derived lymphotoxins are important for recruitment of trafficking cells.^{44,45} It has been debated whether under inflammation, trafficking DCs might be a direct source of chemokines in the DLNs.⁴⁶ In our model, enhanced expression of CCL19 and CCL21 was associated with increased frequencies of graft-derived CD11c⁺ cells and mature CD11c⁺ MHC II⁺ cells in recipients with inflamed graft beds. Sorted and cultured CD11c⁺ cells from the DLNs of recipients with inflamed graft beds secreted significantly higher amounts of CCL19 and CCL21, demonstrating that these DCs directly contribute to the increased CCR7-ligand expression in an inflamed environment. Clinically, recognized high-risk factors for corneal allograft rejection, such as history of infection or other inflammatory conditions,^{1,47–49} may promote allosensitization through enhanced APC trafficking.⁵⁰ Therefore, we propose that targeting mature APC homing through the CCR7-CCL19/21 axis is a potential strategy to reduce graft rejection in high-risk corneal transplantation.

To determine the functional consequences of upregulated CCR7 ligands in the DLNs, we examined the migration of BMDCs toward the supernatant of cultured DLNs from transplant recipients in a transwell migration assay. A significantly greater number of mature BMDCs migrate toward the supernatant collected from DLNs of recipients with an inflamed graft bed than with quiescent graft beds (Supplementary Material S2), and this difference was abolished by blocking CCL19 or CCL21 alone or in combination (Fig. 4A); additionally, serial dilutions of the conditioned media demonstrated a clear dose response in the inflammatory state but no clear trend in the quiescent state (Supplementary Material S2). These results indicate that both CCL19 and CCL21 are involved in enhancing the chemotaxis of mature DCs. Previously, a series of investigations reported that the chemokines CCL19 and CCL21 are preferentially expressed depending on the cell type and disease condition.⁵¹ High endothelial venules of lymph nodes highly express CCL21.^{52,53} Stromal cells in the area surrounding HEVs express CCL19, which is then transported to the lumen of HEVs.⁵³ Based on our observation that the expression of CCR7 on immature DCs was low (Fig. 4B), we speculate that DLNs from recipients with inflamed graft beds selectively recruit mature DCs through expressing high levels of CCR7 ligands (Fig. 3).

Although immunosuppressive agents are used widely to treat inflamed graft beds, in so-called ‘high-risk’ corneal transplantation, they have numerous side effects, and allorecjection remains a substantial clinical problem. We thus performed a series of experiments to determine whether blockade of CCL19 and CCL21 has any additive effect in suppressing DC maturation and function beyond the effect of corticosteroids. Our data show that treatment of BMDCs with dexamethasone decreased their migratory capacity (Figs. 4). Moreover, we observed that blockade of CCL19 and CCL21 further decreased the migration of BMDCs compared with dexamethasone alone (Fig. 4C). Dexamethasone and other immunosuppressive agents have been shown successful in treating transplant rejection.²⁸ Here, we employed dexamethasone as an example of a broad-spectrum anti-inflammatory drug demonstrating that immunosuppression is effective in preventing DC migration. In a previous study we have blocked CCL21 via subconjunctival injection of anti-CCL21

antibody after corneal transplantation and found 40% less CD11c⁺ cells in the DLNs.⁵⁴ Furthermore, it is known that systemic blockade of the CCL19/21-CCR7 axis not only suppresses inflammatory but also immunoregulatory responses.^{55,56} We have thus chosen not to systemically neutralize CCL19 and CCL21 in transplant recipients, because it will effectively interfere regulatory T-cell function.^{56,57}

In summary, our results demonstrate that inflammation at the transplant site promotes trafficking of both recipient- and graft-derived APCs, especially mature CCR7⁺CD11c⁺ DCs, to host lymphoid tissues. Enhanced APC trafficking is due to increased CCL19 and CCL21 secretion in DLNs. The data establish the CCR7-CCL19/21 axis as a key mechanism connecting graft site inflammation with enhanced allosensitization and exacerbated transplant rejection. These results suggest that it is essential to consider the local graft bed inflammatory microenvironment and employ measures that promote local graft bed quiescence to optimize allograft survival.

Acknowledgments

The authors thank Michael Young for providing eGFP mice, Daniel Saban for helpful discussions, Qiang Zhang for technical support, and Susanne Eiglmeier for editorial assistance in the manuscript preparation.

Supported by a grant from the National Institutes of Health (R01 EY12963 RD).

Disclosure: **J. Hua**, None; **W. Stevenson**, None; **T.H. Dohlman**, None; **T. Inomata**, None; **M. Tahvildari**, None; **N. Calcagno**, None; **N. Pirmadjid**, None; **Z. Sadrai**, None; **S.K. Chauhan**, None; **R. Dana**, None

References

1. Dana MR, Qian Y, Hamrah P. Twenty-five-year panorama of corneal immunology: emerging concepts in the immunopathogenesis of microbial keratitis, peripheral ulcerative keratitis, and corneal transplant rejection. *Cornea*. 2000;19:625–643.
2. Niederkorn JY. Corneal transplantation and immune privilege. *Int Rev Immunol*. 2013;32:57–67.
3. Huq S, Liu Y, Benichou G, Dana MR. Relevance of the direct pathway of sensitization in corneal transplantation is dictated by the graft bed microenvironment. *J Immunol*. 2004;173:4464–4469.
4. Hamrah P. High-risk penetrating keratoplasty. *Archivos de la Sociedad Espanola de Oftalmologia*. 2005;80:5–7.
5. Sanfilippo F, MacQueen JM, Vaughn WK, Foulks GN. Reduced graft rejection with good HLA-A and B matching in high-risk corneal transplantation. *N Engl J Med*. 1986;315:29–35.
6. The collaborative corneal transplantation studies (CCTS). Effectiveness of histocompatibility matching in high-risk corneal transplantation. The Collaborative Corneal Transplantation Studies Research Group. *Arch Ophthalmol*. 1992;110:1392–1403.
7. Niederkorn JY. Immune privilege and immune regulation in the eye. *Adv Immunol*. 1990;48:191–226.
8. Sonoda Y, Streilein JW. Orthotopic corneal transplantation in mice—evidence that the immunogenetic rules of rejection do not apply. *Transplantation*. 1992;54:694–704.

9. Joo CK, Pepose JS, Stuart PM. T-cell mediated responses in a murine model of orthotopic corneal transplantation. *Invest Ophthalmol Vis Sci.* 1995;36:1530-1540.
10. Niederkorn JY, Mellon J. Anterior chamber-associated immune deviation promotes corneal allograft survival. *Invest Ophthalmol Vis Sci.* 1996;37:2700-2707.
11. Boisgerault F, Liu Y, Anosova N, Ehrlich E, Dana MR, Benichou G. Role of CD4+ and CD8+ T cells in allorecognition: lessons from corneal transplantation. *J Immunol.* 2001;167:1891-1899.
12. Boisgerault F, Liu Y, Anosova N, Dana R, Benichou G. Differential roles of direct and indirect allorecognition pathways in the rejection of skin and corneal transplants. *Transplantation.* 2009;87:16-23.
13. Morelli AE, Thomson AW. Tolerogenic dendritic cells and the quest for transplant tolerance. *Nat Rev Immunol.* 2007;7:610-621.
14. Lechler R, Ng WF, Steinman RM. Dendritic cells in transplantation—friend or foe? *Immunity.* 2001;14:357-368.
15. Hamrah P, Huq SO, Liu Y, Zhang Q, Dana MR. Corneal immunity is mediated by heterogeneous population of antigen-presenting cells. *J Leukoc Biol.* 2003;74:172-178.
16. Shen L, Barabino S, Taylor AW, Dana MR. Effect of the ocular microenvironment in regulating corneal dendritic cell maturation. *Arch Ophthalmol.* 2007;125:908-915.
17. Huq S, Liu Y, Benichou G, Dana MR. Relevance of the direct pathway of sensitization in corneal transplantation is dictated by the graft bed microenvironment. *J Immunol.* 2004;173:4464-4469.
18. Jin Y, Chauhan SK, Saban DR, Dana R. Role of CCR7 in facilitating direct allosensitization and regulatory T-cell function in high-risk corneal transplantation. *Invest Ophthalmol Vis Sci.* 2010;51:816-821.
19. Jin Y, Shen L, Chong EM, et al. The chemokine receptor CCR7 mediates corneal antigen-presenting cell trafficking. *Mol Vis.* 2007;13:626-634.
20. Forster R, Davalos-Misilitz AC, Rot A. CCR7 and its ligands: balancing immunity and tolerance. *Nat Rev Immunol.* 2008;8:362-371.
21. Mueller SN, Ahmed R. Lymphoid stroma in the initiation and control of immune responses. *Immunol Rev.* 2008;224:284-294.
22. Sano Y, Ksander BR, Streilein JW. Murine orthotopic corneal transplantation in high-risk eyes. Rejection is dictated primarily by weak rather than strong alloantigens. *Invest Ophthalmol Vis Sci.* 1997;38:1130-1138.
23. Liu Y, Hamrah P, Zhang Q, Taylor AW, Dana MR. Draining lymph nodes of corneal transplant hosts exhibit evidence for donor major histocompatibility complex (MHC) class II-positive dendritic cells derived from MHC class II-negative grafts. *J Exp Med.* 2002;195:259-268.
24. Murphy DB, Lo D, Rath S, et al. A novel MHC class II epitope expressed in thymic medulla but not cortex. *Nature.* 1989;338:765-768.
25. Ochando JC, Krieger NR, Bromberg JS. Direct versus indirect allorecognition: visualization of dendritic cell distribution and interactions during rejection and tolerization. *Am J Transplant.* 2006;6:2488-2496.
26. Inaba K, Inaba M, Deguchi M, et al. Granulocytes, macrophages, and dendritic cells arise from a common major histocompatibility complex class II-negative progenitor in mouse bone marrow. *Proc Natl Acad Sci U S A.* 1993;90:3038-3042.
27. Larange A, Antonios D, Pallardy M, Kerdine-Romer S. Glucocorticoids inhibit dendritic cell maturation induced by Toll-like receptor 7 and Toll-like receptor 8. *J Leukoc Biol.* 2012;91:105-117.
28. Ziaei M, Manzouri B. Topical cyclosporine in corneal transplantation. *Cornea.* 2015;34:110-115.
29. Kuffova L, Netukova M, Duncan L, Porter A, Stockinger B, Forrester JV. Cross presentation of antigen on MHC class II via the draining lymph node after corneal transplantation in mice. *J Immunol.* 2008;180:1353-1361.
30. Steptoe RJ, Li W, Fu F, O'Connell PJ, Thomson AW. Trafficking of APC from liver allografts of Flt3L-treated donors: augmentation of potent allostimulatory cells in recipient lymphoid tissue is associated with a switch from tolerance to rejection. *Transpl Immunol.* 1999;7:51-57.
31. Blanco P, Palucka AK, Pascual V, Banchereau J. Dendritic cells and cytokines in human inflammatory and autoimmune diseases. *Cytokine Growth Factor Rev.* 2008;19:41-52.
32. Yamada J, Dana MR, Zhu SN, Alard P, Streilein JW. Interleukin 1 receptor antagonist suppresses allosensitization in corneal transplantation. *Arch Ophthalmol.* 1998;116:1351-1357.
33. Dana MR, Yamada J, Streilein JW. Topical interleukin 1 receptor antagonist promotes corneal transplant survival. *Transplantation.* 1997;63:1501-1507.
34. Dekaris JJ, Yamada JJ, Streilein WJ, Dana RM. Effect of topical interleukin-1 receptor antagonist (IL-1ra) on corneal allograft survival in presensitized hosts. *Curr Eye Res.* 1999;19:456-459.
35. Dana R. Comparison of topical interleukin-1 vs tumor necrosis factor-alpha blockade with corticosteroid therapy on murine corneal inflammation, neovascularization, and transplant survival (an American Ophthalmological Society thesis). *Trans Am Ophthalmol Soc.* 2007;105:330-343.
36. Forster R, Schubel A, Breitfeld D, et al. CCR7 coordinates the primary immune response by establishing functional microenvironments in secondary lymphoid organs. *Cell.* 1999;99:23-33.
37. Tal O, Lim HY, Gurevich I, et al. DC mobilization from the skin requires docking to immobilized CCL21 on lymphatic endothelium and intralymphatic crawling. *J Exp Med.* 2011;208:2141-2153.
38. Hamrah P, Zhang Q, Liu Y, Dana MR. Novel characterization of MHC class II-negative population of resident corneal Langerhans cell-type dendritic cells. *Invest Ophthalmol Vis Sci.* 2002;43:639-646.
39. Girard JP, Moussion C, HEVs, Forster R. lymphatics and homeostatic immune cell trafficking in lymph nodes. *Nat Rev Immunol.* 2012;12:762-773.
40. Ngo VN, Korner H, Gunn MD, et al. Lymphotoxin alpha/beta and tumor necrosis factor are required for stromal cell expression of homing chemokines in B and T cell areas of the spleen. *J Exp Med.* 1999;189:403-412.
41. Fava RA, Kennedy SM, Wood SG, et al. Lymphotoxin-beta receptor blockade reduces CXCL13 in lacrimal glands and improves corneal integrity in the NOD model of Sjogren's syndrome. *Arthritis Res Ther.* 2011;13:R182.
42. McNamee EN, Masterson JC, Jedlicka P, Collins CB, Williams IR, Rivera-Nieves J. Ectopic lymphoid tissue alters the chemokine gradient, increases lymphocyte retention and exacerbates murine ileitis. *Gut.* 2013;62:53-62.
43. Sanchez-Nino MD, Benito-Martin A, Goncalves S, et al. TNF superfamily: a growing saga of kidney injury modulators. *Mediators Inflamm.* 2010;2010:pii:182958.
44. Moussion C, Girard JP. Dendritic cells control lymphocyte entry to lymph nodes through high endothelial venules. *Nature.* 2011;479:542-546.
45. Wendland M, Willenzon S, Kocks J, et al. Lymph node T cell homeostasis relies on steady state homing of dendritic cells. *Immunity.* 2011;35:945-957.
46. Girard JP, Moussion C, HEVs, Forster R. lymphatics and homeostatic immune cell trafficking in lymph nodes. *Nat Rev Immunol.* 2012;12:762-773.

47. Lomholt JA, Ehlers N. Graft survival and risk factors of penetrating keratoplasty for microbial keratitis. *Acta Ophthalmol Scand*. 1997;75:418-422.
48. Constantinou M, Jhanji V, Vajpayee RB. Clinical and microbiological profile of post-penetrating keratoplasty infectious keratitis in failed and clear grafts. *Am J Ophthalmol*. 2013;155:233-237, e232.
49. Anshu A, Lim LS, Htoon HM, Tan DT. Postoperative risk factors influencing corneal graft survival in the Singapore Corneal Transplant Study. *Am J Ophthalmol*. 2011;151:442-448, e441.
50. Ato M, Maroof A, Zubairi S, Nakano H, Kakiuchi T, Kaye PM. Loss of dendritic cell migration and impaired resistance to *Leishmania donovani* infection in mice deficient in CCL19 and CCL21. *J Immunol*. 2006;176:5486-5493.
51. Forster R, Davalos-Missslitz AC, Rot A. CCR7 and its ligands: balancing immunity and tolerance. *Nat Rev Immunol*. 2008;8:362-371.
52. Gunn MD, Tangemann K, Tam C, Cyster JG, Rosen SD, Williams LT. A chemokine expressed in lymphoid high endothelial venules promotes the adhesion and chemotaxis of naive T lymphocytes. *Proc Natl Acad Sci U S A*. 1998;95:258-263.
53. Miyasaka M, Tanaka T. Lymphocyte trafficking across high endothelial venules: dogmas and enigmas. *Nat Rev Immunol*. 2004;4:360-370.
54. Jin Y, Shen L, Chong EM, et al. The chemokine receptor CCR7 mediates corneal antigen-presenting cell trafficking. *Mol Vis*. 2007;13:626-634.
55. Liu X, Mishra P, Yu S, et al. Tolerance induction towards cardiac allografts under costimulation blockade is impaired in CCR7-deficient animals but can be restored by adoptive transfer of syngeneic plasmacytoid dendritic cells. *Eur J Immunol*. 2011;41:611-623.
56. Jin Y, Chauhan SK, Saban DR, Dana R. Role of CCR7 in facilitating direct allosensitization and regulatory T-cell function in high-risk corneal transplantation. *Invest Ophthalmol Vis Sci*. 2010;51:816-821.
57. Chauhan SK, Saban DR, Dohlman TH, Dana R. CCL-21 conditioned regulatory T cells induce allotolerance through enhanced homing to lymphoid tissue. *J Immunol*. 2014;192:817-823.
58. Vassileva G, Soto H, Zlotnik A, et al. The reduced expression of 6Ckine in the plt mouse results from the deletion of one of two 6Ckine genes. *J Exp Med*. 1999;190:1183-1188.